



Contents lists available at ScienceDirect

## Journal of Magnetic Resonance

journal homepage: [www.elsevier.com/locate/jmr](http://www.elsevier.com/locate/jmr)

## Communication

## NMR at earth's magnetic field using para-hydrogen induced polarization

Bob C. Hamans<sup>a,\*</sup>, Anna Andreychenko<sup>b,2,3</sup>, Arend Heerschap<sup>a,1</sup>, Sybren S. Wijmenga<sup>b,2</sup>, Marco Tessari<sup>b,2</sup><sup>a</sup> Department of Radiology, Radboud University Nijmegen Medical Centre, Geert Grooteplein 10, 6525 GA Nijmegen, The Netherlands<sup>b</sup> Institute for Molecules and Materials, Radboud University Nijmegen, Heyendaalseweg 135, 6525 AJ Nijmegen, The Netherlands

## ARTICLE INFO

## Article history:

Received 13 April 2011

Revised 8 June 2011

Available online 20 July 2011

## Keywords:

Earth field

NMR

Hydrogenation

Field cycling

Parahydrogen

## ABSTRACT

A method to achieve NMR of dilute samples in the earth's magnetic field by applying para-hydrogen induced polarization is presented. Maximum achievable polarization enhancements were calculated by numerically simulating the experiment and compared to the experimental results and to the thermal equilibrium in the earth's magnetic field. Simultaneous <sup>19</sup>F and <sup>1</sup>H NMR detection on a sub-milliliter sample of a fluorinated alkyne at millimolar concentration ( $\sim 10^{18}$  nuclear spins) was realized with just one single scan. A highly resolved spectrum with a signal/noise ratio higher than 50:1 was obtained without using an auxiliary magnet or any form of radio frequency shielding.

© 2011 Elsevier Inc. All rights reserved.

## 1. Introduction

NMR spectroscopy is a powerful analytical tool for non-destructive investigations in material science, chemistry and biology. The resolving power of the technique depends on the chemical shift dispersion, which is linearly dependent on the magnetic field strength. Recent applications of low field NMR [1–3] nevertheless demonstrated the possibility of obtaining analytical information in the absence of strong magnetic fields. In contrast to using chemical shift, as is common in high field NMR, the information at low field is obtained from heteronuclear couplings resolved with high accuracy. The main disadvantage of NMR at such low fields is its inherent low sensitivity; therefore, concentrated samples (typically  $10^{21}$ – $10^{25}$  nuclear spins) pre-polarized at higher magnetic fields are required.

The aim of this study was to develop a method to measure low field NMR on dilute samples by exploiting the sensitivity gain provided by nuclear spin hyperpolarization. Several techniques [4–7] are nowadays available to increase the population differences of the nuclear spin states far beyond thermal equilibrium. Here, we present a theoretical description and report on the results of an NMR measurement performed at earth's field, using Para-Hydrogen

Induced Polarization [8–10] (PHIP) as hyperpolarization method. The NMR data we present have been acquired with just one scan on a sub-milliliter sample at millimolar concentration ( $\sim 10^{18}$  nuclear spins).

## 2. Theory

PHIP requires a fast chemical reaction between the para-spin isomer of molecular hydrogen (*p*-H<sub>2</sub>) and an organic substrate (typically an alkene or an alkyne) [4–6,8,11]. Depending on the magnetic field strength during the hydrogenation, PHIP experiments are classified as PASADENA [8,11,12] (high field) or ALTADENA [9,13] (low field). Recently, optimized versions of PHIP have been proposed relying on RF irradiation [10,14] or magnetic field cycling (FC) [13,15] to convert the proton spin order of the *p*-hydrogenated product into longitudinal magnetization. Noticeably, nuclear hyperpolarization has been recently obtained also via reversible association of an organic substrate with *p*-H<sub>2</sub> [16], thereby lifting the stringent requirement of a *p*-hydrogenation reaction.

The conversion of spin order to proton and heteronuclear longitudinal magnetization in a FC experiment has been discussed in the original paper of Jóhannesson et al. [15]. In Fig. 1A we summarize his conclusions for the specific case of a <sup>1</sup>H, <sup>19</sup>F spin system. For simplicity we present a reduced spin system consisting of two protons from *p*-H<sub>2</sub> and a single <sup>19</sup>F nuclear spin. The energy diagrams in Fig. 1A were drawn considering a 100% *p*-H<sub>2</sub> enrichment and assuming the same scalar coupling network (<sup>3</sup>J<sub>HH</sub> = 12.5 Hz, <sup>3</sup>J<sub>HF</sub> = 8.4 Hz, <sup>4</sup>J<sub>HF</sub>  $\sim$  -0.8 Hz) as found in the hydrogenated product, 4,4,4-trifluoro but-2-enoate, used in the experiment

\* Corresponding author. Fax: +31 24 3540866.

E-mail addresses: [b.hamans@rad.umcn.nl](mailto:b.hamans@rad.umcn.nl) (B.C. Hamans), [a.andreychenko@umcutrecht.nl](mailto:a.andreychenko@umcutrecht.nl) (A. Andreychenko), [a.heerschap@rad.umcn.nl](mailto:a.heerschap@rad.umcn.nl) (A. Heerschap), [s.wijmenga@science.ru.nl](mailto:s.wijmenga@science.ru.nl) (S.S. Wijmenga), [m.tessari@science.ru.nl](mailto:m.tessari@science.ru.nl) (M. Tessari).<sup>1</sup> Fax: +31 24 3540866.<sup>2</sup> Fax: +31 24 3652112.<sup>3</sup> Present address: Image Science Institute, University Medical Center Utrecht, Heidelberglaan 100, 3584 CX Utrecht, The Netherlands.

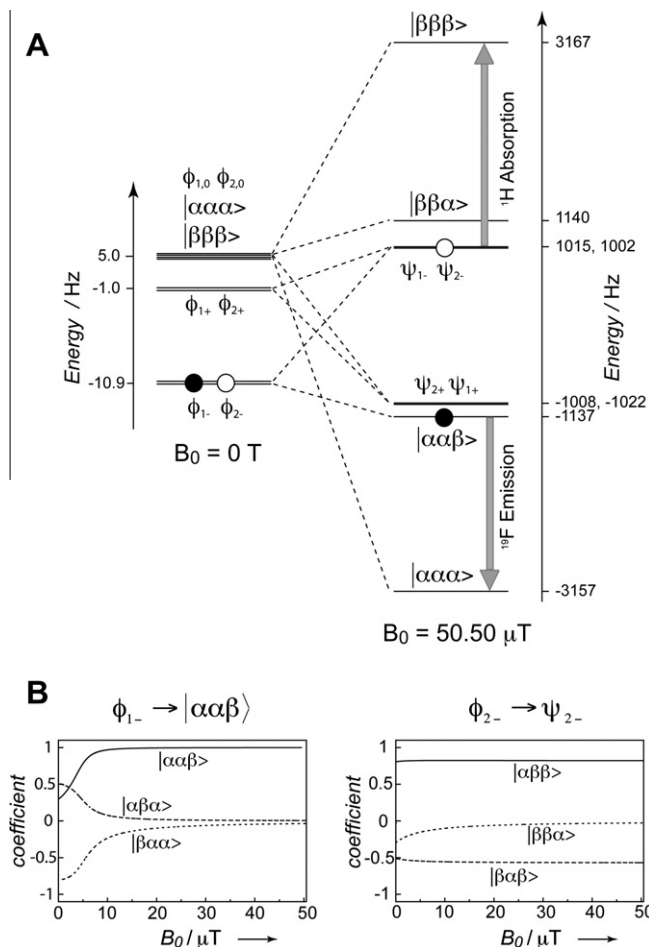


**Fig. 1.** (A) Energy diagram at zero field and at earth's field ( $50.50 \mu\text{T}$ ) of a ( $^1\text{H}$ ,  $^{19}\text{F}$ ) spin system; the energy values were calculated assuming the same H–H and H–F coupling constants as found in 4,4,4-trifluoro but-2-enoate and by using the expressions given in Ref. [15]. The populations of the  $\phi_{1-}$  and  $\phi_{2-}$  eigenstates are represented with a black and white circle, respectively. The gray arrows indicate the transitions corresponding to the signals observed in the earth's field NMR spectrum (B) Field dependence of the coefficients defining the eigenstates  $\phi_{1-}$  (left) and  $\phi_{2-}$  (right) in the Zeeman eigenbasis.

(see below). The eigenstates at zero field and earth's field ( $\gamma B_0/2\pi$ :  $^1\text{H} = 2152 \text{ Hz}$ ,  $^{19}\text{F} = 2020 \text{ Hz}$ ) are expressed below in the Zeeman eigenbasis; expressions for the value of the coefficients can be found in [15].

$$\begin{aligned}
 \phi_{1-} &= c_1^- |\alpha\alpha\beta\rangle + c_2^- |\alpha\beta\alpha\rangle + c_3^- |\beta\alpha\alpha\rangle \\
 \phi_{2-} &= c_1^- |\beta\beta\alpha\rangle + c_2^- |\beta\alpha\beta\rangle + c_3^- |\alpha\beta\beta\rangle \\
 \phi_{1+} &= c_1^+ |\alpha\alpha\beta\rangle + c_2^+ |\alpha\beta\alpha\rangle + c_3^+ |\beta\alpha\alpha\rangle \\
 \phi_{2+} &= -c_1^+ |\beta\beta\alpha\rangle - c_2^+ |\beta\alpha\beta\rangle - c_3^+ |\alpha\beta\beta\rangle \\
 \phi_{1,0} &= \frac{1}{\sqrt{3}} (|\alpha\alpha\beta\rangle + |\alpha\beta\alpha\rangle + |\beta\alpha\alpha\rangle) \\
 \phi_{2,0} &= \frac{1}{\sqrt{3}} (|\beta\beta\alpha\rangle + |\beta\alpha\beta\rangle + |\alpha\beta\beta\rangle) \\
 &|\alpha\alpha\alpha\rangle, |\beta\beta\beta\rangle
 \end{aligned} \quad (1)$$

at zero field and

$$\begin{aligned}
 \psi_{1-} &= c_- |\alpha\beta\alpha\rangle + c_+ |\beta\alpha\alpha\rangle \\
 \psi_{2-} &= c_+ |\alpha\beta\beta\rangle + c_- |\beta\alpha\beta\rangle \\
 \psi_{1+} &= c_+ |\alpha\beta\alpha\rangle - c_- |\beta\alpha\alpha\rangle \\
 \psi_{2+} &= c_- |\alpha\beta\beta\rangle + c_+ |\beta\alpha\beta\rangle \\
 &|\alpha\alpha\beta\rangle, |\beta\beta\alpha\rangle, |\alpha\alpha\alpha\rangle, |\beta\beta\beta\rangle
 \end{aligned} \quad (2)$$

at earth's field.

After  $p$ -hydrogenation and sudden jump to zero field, only energy levels corresponding to eigenstates with a total magnetic quantum number  $M_z = +/ - \frac{1}{2}$  are populated [15]. For an in-depth discussion about the eigenstates of a three-spin system at low-field and the population distribution after  $p$ -hydrogenation see [17,18]. The population distribution within these energy levels depends on the strength of H–H as well as H–F scalar coupling interactions. In the case of our spin system, ca. 80% of the total population is equally distributed between the  $\phi_{1-}$  and  $\phi_{2-}$  eigenstates (circles black and white in Fig. 1A). For the sake of clarity, the remaining 20% population (almost uniformly distributed among the other energy levels) is not displayed in Fig. 1A and not further considered.

During adiabatic remagnetization, the eigenstates smoothly follow the Hamiltonian change while the populations of the corresponding energy levels are left unperturbed. As a consequence, only two energy levels remain considerably populated during the whole remagnetization process.

The eigenstates transformation from zero field to earth's field can be followed by numerical methods. In Fig. 1B, the conversion of the two highly populated eigenstates at zero field (i.e.  $\phi_{1-}$  and  $\phi_{2-}$ ) is shown.  $\phi_{1-}$  (black circle) transforms to  $|\alpha\alpha\beta\rangle$ , in agreement with the emissive  $^{19}\text{F}$  signal in the earth's field NMR spectrum of Fig. 3, which corresponds to the transition  $|\alpha\alpha\beta\rangle \rightarrow |\alpha\alpha\alpha\rangle$ . In contrast,  $\phi_{2-}$  (white circle) transforms to eigenstate  $\psi_{2-}$ : this is consistent with the  $^1\text{H}$  absorptive signal in the earth's field NMR spectrum of Fig. 3, originating from the transition  $\psi_{2-} \rightarrow |\beta\beta\beta\rangle$ .

The optimal magnetic field profile during remagnetization depends on the scalar coupling network as well as on the gyromagnetic ratios of the nuclear spins in the  $p$ -hydrogenated molecules. Adiabatic remagnetization of ( $^1\text{H}$ ,  $^{13}\text{C}$ ) spin systems has been previously achieved with a linear or exponential profile of approximately 1–5 s duration [15,19]. In the present case, where both  $^1\text{H}$  and  $^{19}\text{F}$  T1 relaxation times at earth's field are on the order of 1 s, a faster remagnetization is desirable. We therefore calculated the shortest possible remagnetization trajectory satisfying the general requirements posed by the approximate adiabatic criterion [20,21] within a 0.01 tolerance (see below). The time dependence of the magnetic field during remagnetization was determined for the hyperpolarized spin system of 4,4,4-trifluoro but-2-enoate (i.e. three equivalent  $^{19}\text{F}$  spins and two  $^1\text{H}$  spins). The ramp from low to high field (Fig. 2A) was divided in 100 steps of equal amplitude; the duration of each individual step was determined under the condition that the transition probability between any pair of eigenvectors [20] be less than 0.01. Our approach resulted in a remagnetization profile of approximately 210 ms, substantially shorter than  $^1\text{H}$  and  $^{19}\text{F}$  T1. The nuclear magnetization for  $^1\text{H}$  and  $^{19}\text{F}$  during the remagnetization, calculated under the assumption of an adiabatic process, is shown in Fig. 2B (dashed curve): a spin polarization of ca. 60% (i.e. twice the expectation value  $\langle I_z \rangle$ , see [15]) is predicted for both nuclear species at the end of the trajectory. Comparable results were obtained by numerically solving the Liouville–von Neumann equation to determine the evolution of the density matrix during the remagnetization. The oscillations of the longitudinal magnetization displayed in Fig. 2B (full curve) are due to the evolution of off-diagonal terms of the density matrix [10]. Given the short duration of the remagnetization the effects of longitudinal- and cross relaxation were assumed negligible and, therefore, not included in the calculation.

### 3. Experimental results and discussion

Hyperpolarization of both  $^1\text{H}$  and  $^{19}\text{F}$  nuclear spins was obtained using a diabatic-adiabatic field cycling (FC) scheme [15] following  $p$ -hydrogenation. We chose a fluorinated compound as it allows for simultaneous detection of both hyperpolarized nuclear

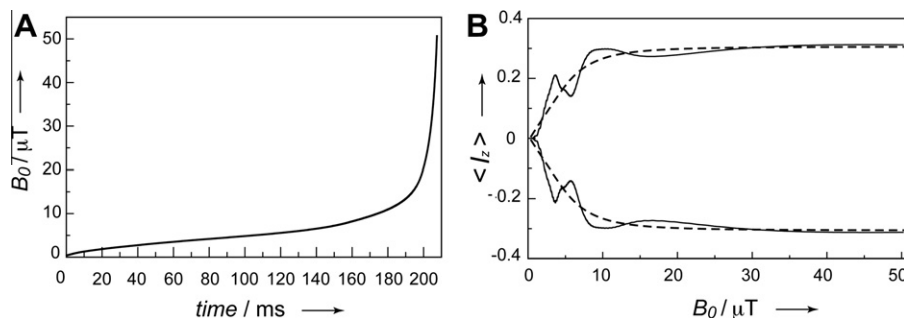


**Fig. 2.** (A) Profile of the magnetic field strength  $B_0$  versus time for the adiabatic remagnetization. The curve was calculated with a 0.01 tolerance (see text). (B) Buildup of  $^1\text{H}$  and  $^{19}\text{F}$  longitudinal magnetization during the remagnetization assuming an adiabatic process (dashed) or solving the Liouville–von Neumann equation in steps of  $20\ \mu\text{s}$  (full). The calculations were carried out neglecting the effects of spin relaxation and assuming a  $p\text{-H}_2$  enrichment of 80% as used for the experiment (see below).

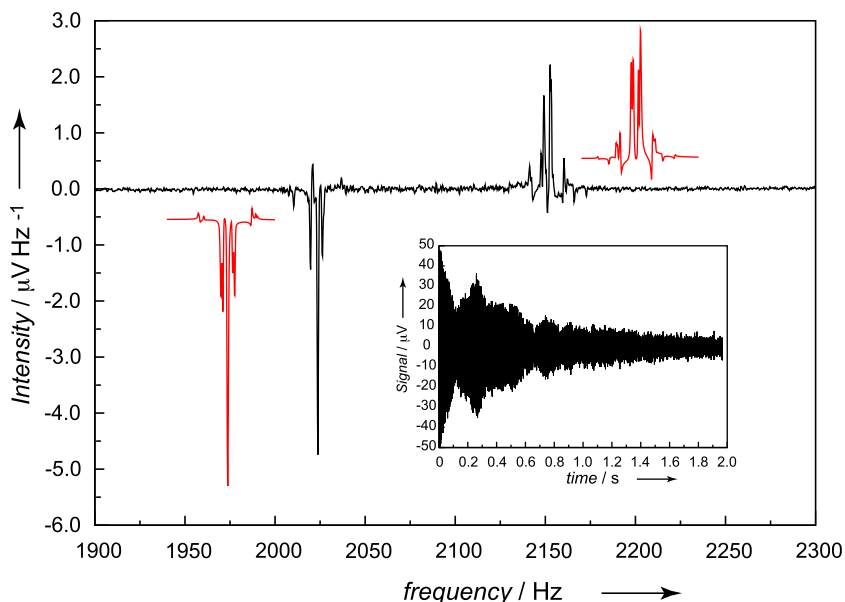


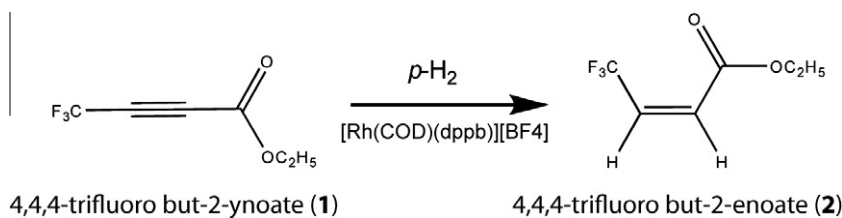
**Fig. 3.** Single-scan earth's field NMR spectrum (in black) of  $310\ \mu\text{l}$  hyperpolarized 4,4,4-trifluoro but-2-enoate (2), 9 mM in perdeuterated acetone. A signal/noise ratio higher than 50:1 was estimated from peak intensities and RMSD noise of the spectrum ( $0.03\ \mu\text{V}/\text{Hz}$ ). The multiplets displayed in red are obtained by simulating the complete field cycling experiment (i.e. para-hydrogenation + adiabatic remagnetization + excitation + detection at earth's magnetic field). Inset: FID acquired at earth field ( $50.50\ \mu\text{T}$ ) after hydrogenation of 4,4,4-trifluoro but-2-ynoate (1) with 80% enriched parahydrogen and diabatic-adiabatic field cycling.  $^1\text{H}$  and  $^{19}\text{F}$  signals were acquired for 2 s after a RF pulse of 0.7 ms, corresponding to a  $\sim 90^\circ$  flip angle, and with a pre-acquisition delay of 25 ms.

species at earth field [22]. We could therefore compare the attained hetero nuclear polarizations and validate our results against our theoretical prediction. In addition, our choice simplified the experimental setup as the  $^1\text{H}$ – $^{19}\text{F}$  strong coupling condition required during the field cycling (see above) can be achieved already at magnetic field strengths of a few microTesla.

The NMR sample we used consisted of  $310\ \mu\text{l}$  of oxygen-free solution of 4,4,4-trifluoro but-2-enoate (2) 9 mM in deuterated acetone. It was obtained by  $p$ -hydrogenation of 4,4,4-trifluoro but-2-ynoate (1) using 15 mM [Rh(cyclo-octadiene) diphenyl-

phosphanyl butane] [BF<sub>4</sub>] as catalyst and 80% enriched  $p\text{-H}_2$  at 0.2 MPa (2 bars). The reaction (Scheme 1) was carried out in 5 s, resulting in a 95% yield, as established by conventional high field  $^1\text{H}$  NMR after the earth's field (EF) NMR experiment.

An NMR spectrum of 4,4,4-trifluoro but-2-enoate (2) with signals substantially above the noise level was acquired at earth's field ( $50.5\ \mu\text{T}$ ) in a single scan (Fig. 3). Two signals with comparable integrals and opposite sign are found in the spectrum, experimentally confirming the prediction about opposite polarizations reported earlier [15]. The multiplet structure of  $^1\text{H}$  and  $^{19}\text{F}$  signals



**Scheme 1.** Production of 4,4,4-trifluoro but-2-enoate (2) from 4,4,4-trifluoro but-2-ynoate (1).

results from H–H and H–F couplings ( $^3J_{\text{HH}} = 12.5$  Hz,  $^3J_{\text{HF}} = 8.4$  Hz,  $^4J_{\text{HF}} \sim -0.8$  Hz). The two signals roughly resemble a quartet and a triplet with a splitting of ca. 3.5 Hz. A more careful analysis of these “deceptively simple” structures [23] reveals a complex peak pattern, consistent with the H–H (and partially H–F) strong coupling regime. A linewidth of  $\sim 0.7$  Hz was estimated for the multiplets components, illustrating the magnetic field homogeneity within the sample. This is quite remarkable, considering that the spectrum was acquired indoor without sample shimming, in close proximity to armed concrete floor and ceiling. The shape and relative intensity of the two multiplets is in very good agreement with the result of a simulation of the complete FC experiment (Fig. 3 in red<sup>4</sup>), using standard propagation methods (relaxation not included). This supports the notion of scalar-couplings [15,24,25], rather than cross-relaxation, as being the driving force of the hyperpolarization process by diabatic FC.

The core of the NMR setup consists of a solenoid coil used for RF excitation and signal detection. The solution containing 4,4,4-trifluoro but-2-ynoate (1) was centered on the axis of this coil in a small glass sphere (ca. 350  $\mu\text{l}$ ) connected to an evacuated chamber of ca. 12 ml. Whilst placed inside the coil this reaction chamber was instantaneously filled with 80% enriched *p*-H<sub>2</sub> to form 4,4,4-trifluoro but-2-enoate (2). After the *p*-hydrogenation, the magnetic field was reduced from 150  $\mu\text{T}$  to approximately zero field ( $<3$   $\mu\text{T}$ ) in less than 1 ms. The field strength was then adiabatically increased up to earth's field. During the adiabatic remagnetization the spin order originating from *p*-H<sub>2</sub> evolves coherently in <sup>19</sup>F and <sup>1</sup>H longitudinal magnetization. RF irradiation and signal detection take place in situ, with no additional dead time for sample transfer. While non-inductive detection systems (e.g. SQUID [1]) could have offered a higher sensitivity, we have here privileged the simplicity and portability of a conventional inductive coil.

The spin polarization experimentally obtained using the calculated magnetic field profile, was estimated by comparison with the earth's field <sup>1</sup>H NMR spectrum of a sample of 3.9 ml water ( $\sim 10^{23}$  proton spins). This reference spectrum was acquired in 16 scans, repetitively polarizing the water protons at 15  $\mu\text{T}$  for 5 s, while keeping all other experimental parameters unchanged. From the comparison of the signal integrals, a spin polarization of ca. 3% was estimated for both <sup>1</sup>H and <sup>19</sup>F, corresponding to a 108-fold polarization enhancement with respect to thermal equilibrium. In part, the discrepancy with the (20 times larger) predicted enhancement might be explained in terms of singlet–triplet mixing during the reaction, which converts the long-lived state originating from *p*-H<sub>2</sub> [18] into faster relaxing terms (i.e. H–F longitudinal spin order). Such interconversion between singlet and triplet states could be prevented by selective proton irradiation [10,26,27] during the reaction.

#### 4. Conclusion

A method to measure earth's field NMR on dilute samples, exploiting the sensitivity gain provided by PHIP, was presented. PHIP dramatically lowers the requirements for earth's field NMR to sample volumes and concentrations common to high field NMR investigations. The method has enabled us to measure earth's field NMR even under non-ideal conditions (e.g. indoor and using a conventional coil).

#### 5. Experimental

Para-hydrogen (*p*-H<sub>2</sub>) was produced at 20 K in the presence of iron oxide and stored at a pressure of 0.2 MPa (2 bars) in an alumi-

num bottle for later use [28]. The level of *p*-H<sub>2</sub> enrichment was assessed by recording a high field <sup>1</sup>H NMR spectrum using a Varian UnityNOVA (500 MHz, <sup>1</sup>H frequency) before starting the earth's field NMR experiment.

For NMR a B1 and an optional polarization coil were positioned exactly in the isocentre of a Helmholtz pair. The magnetic field strength through the sample was modified with the Helmholtz pair, oriented approximately 67° from the horizontal plane set to produce a magnetic field parallel or opposite to the earth's magnetic field. The accuracy of the alignment between earth's magnetic field and the Helmholtz field was determined not to be better than 2.7°, which determined a small field component oriented perpendicular to the earth's magnetic field. Numerical simulations indicate a modest decrease (ca. 5%) of <sup>1</sup>H and <sup>19</sup>F spin polarization at the end of the remagnetization step due to this residual magnetic field (approximately 2  $\mu\text{T}$ , corresponding to  $v(^1\text{H}) - v(^{19}\text{F}) \sim 6$  Hz immediately after the jump from earth field to low field). The setup allows for in situ measurement of NMR spectra, without additional “dead periods” for sample transfer to an NMR spectrometer.

Chemicals were purchased from Sigma–Aldrich. Care was taken to degas all chemicals and glassware used in the experiment. For activation 160  $\mu\text{l}$  of the catalyst solution was injected into the evacuated reactor and pressurized with 0.2 MPa (2 bars) H<sub>2</sub>. After 60 s of gentle mixing the catalyst was assumed activated and the reactor was evacuated once more before introducing 150  $\mu\text{l}$  of the substrate solution.

Before starting the para-hydrogenation reaction and field cycling experiment the reactor, now containing the activated catalyst and substrate, was connected to the *p*-H<sub>2</sub> vessel (0.2 MPa/2 bars) and inserted into the NMR coil setup (see above).

Immediately after the remagnetization, performed using the calculated adiabatic trajectory (see above), an NMR spectrum of the hydrogenated product was acquired at earth's field.

The NMR spectrum of the hydrogenated product was acquired following a 0.7 ms ( $\sim 90^\circ$ ) RF pulse at a frequency of 2090 Hz (exactly between <sup>19</sup>F and <sup>1</sup>H Larmor frequencies at earth's field) and a 25 ms B1 coil ring-down delay. Total acquisition time was 2 s in which a total of 32 k real points was recorded. The free induction decay (FID) was processed with scripts implemented in MATLAB<sup>®</sup> using 90° shifted square sine-bell apodization, prior to zero-filling to 64 k real points, and Fourier transformation.

The evolution of the hyperpolarized spin system during field cycling, RF irradiation and detection period was calculated by standard propagation methods, with a full non-truncated Hamiltonian. The simulation was carried out as numerical integration of the Liouville time-dependent differential equations in constant time steps of 20  $\mu\text{s}$  (for the 210 ms adiabatic remagnetization), 0.7  $\mu\text{s}$  (for the 0.7 ms RF pulse) and 200  $\mu\text{s}$  (for the acquisition period) using MATLAB<sup>®</sup>. The effects of relaxation were not accounted for in these simulations. The calculated FID was processed in a similar fashion as the acquired FID (see above).

#### Acknowledgments

Jan van Os, Peter Walraven and Dr. Craig Eccles (Magritek Ltd) are gratefully acknowledged for technical and software support, prof. Dave Parker and prof. Wim van der Zande for a gift of enriched *p*-H<sub>2</sub> and Dr. Andreas Brinkmann for stimulating discussions.

#### References

- [1] R. McDermott, A.H. Trabesinger, M. Muck, E.L. Hahn, A. Pines, J. Clarke, *Science* 295 (2002) 2247–2249.
- [2] S. Appelt, H. Kühn, F.W. Häsing, B. Blümich, *Nat. Phys.* 2 (2006) 105–109.

<sup>4</sup> For interpretation of color in Fig. 3, the reader is referred to the web version of this article.

- [3] C.M. Thiele, *Angew. Chem., Int. Ed.* 46 (2007) 4820–4824.
- [4] M.G. Pravica, D.P. Weitekamp, *Chemical Physics Letters* 145 (1988) 255–258.
- [5] L.T. Kuhn, U. Bommerich, J. Bargon, *J. Phys. Chem. A* 110 (2006) 3521–3526.
- [6] C.R. Bowers, in: D.M. Grant, R.K. Harris (Eds.), *Encyclopedia of Nuclear Magnetic Resonance*, 2002, pp. 750–770.
- [7] T.G. Walker, W. Happer, *Rev. Mod. Phys.* 69 (1997) 629.
- [8] C.R. Bowers, D.P. Weitekamp, *J. Am. Chem. Soc.* 109 (1987) 5541–5542.
- [9] S. Aime, R. Gobetto, F. Reineri, D. Canet, *J. Chem. Phys.* 119 (2003) 8890.
- [10] M. Goldman, H. Jóhannesson, O. Axelsson, M. Karlsson, *C.R. Chim.* 9 (2006) 357–363.
- [11] C.R. Bowers, D.P. Weitekamp, *Phys. Rev. Lett.* 57 (1986) 2645.
- [12] E.Y. Chekmenev, J. Hövener, V.A. Norton, K. Harris, L.S. Batchelder, P. Bhattacharya, B.D. Ross, D.P. Weitekamp, *J. Am. Chem. Soc.* 130 (2008) 4212–4213.
- [13] U. Bommerich, T. Trantzscheil, S. Mulla-Osman, G. Buntkowsky, J. Bargon, J. Bernarding, *Phys. Chem. Chem. Phys.* 12 (2010) 10309.
- [14] M. Haake, J. Natterer, J. Bargon, *J. Am. Chem. Soc.* 118 (1996) 8688–8691.
- [15] H. Jóhannesson, O. Axelsson, M. Karlsson, *C.R. Phys.* 5 (2004) 315–324.
- [16] R.W. Adams, J.A. Aguilar, K.D. Atkinson, M.J. Cowley, P.I.P. Elliott, S.B. Duckett, G.G.R. Green, I.G. Khazal, J. Lopez-Serrano, D.C. Williamson, *Science* 323 (2009) 1708–1711.
- [17] A.K. Grant, E. Vinogradov, *J. Magn. Reson.* 193 (2008) 177–190.
- [18] E. Vinogradov, A.K. Grant, *J. Magn. Reson.* 194 (2008) 46–57.
- [19] F. Reineri, A. Viale, G. Giovenzana, D. Santelia, W. Dastrù, R. Gobetto, S. Aime, *J. Am. Chem. Soc.* 130 (2008) 15047–15053.
- [20] A. Messiah, *Quantum Mechanics*, vols. I and II, Dover Publications, Mineola, New York, United States of America, 1961.
- [21] D. Comparat, *Phys. Rev. A* 80 (2009) 012106.
- [22] M.E. Halse, P.T. Callaghan, *J. Magn. Reson.* 195 (2008) 162–168.
- [23] E.D. Becker, *High Resolution NMR: Theory and Chemical Applications*, Academic Press, 2000.
- [24] S.E. Korchak, K.L. Ivanov, A.V. Yurkovskaya, H.-M. Vieth, *Phys. Chem. Chem. Phys.* 11 (2009) 11146–11156.
- [25] L. Kuhn, J. Bargon, *In Situ NMR Methods in Catalysis*, 2007, pp. 25–68.
- [26] G. Pileio, M.H. Levitt, *J. Chem. Phys.* 130 (2009) 214501–214514.
- [27] P.R. Vasos, A. Comment, R. Sarkar, P. Ahuja, S. Jannin, J.-P. Ansermet, J.A. Konter, P. Hautle, B. van den Brandt, G. Bodenhausen, *Proc. Natl. Acad. Sci. U.S.A.* 106 (2009) 18469–18473.
- [28] K.F. Bonhoeffer, P. Harteck, *Naturwissenschaften* 17 (1929) 182.